

## A nonlinear structural experiment platform with adjustable plastic hinges: analysis and vibration control

Luyu Li<sup>1,2</sup>, Gangbing Song<sup>\*1,2</sup> and Jinping Ou<sup>2</sup>

<sup>1</sup>Department of Mechanical Engineering, University of Houston, Houston, TX, USA

<sup>2</sup>School of Civil Engineering, Dalian University of Technology, Dalian, P.R. China

(Received June 11, 2012, Revised November 25, 2012, Accepted November 30, 2012)

**Abstract.** The construction of an experimental nonlinear structural model with little cost and unlimited repeatability for vibration control study represents a challenging task, especially for material nonlinearity. This paper reports the design, analysis and vibration control of a nonlinear structural experiment platform with adjustable hinges. In our approach, magnetorheological rotary brakes are substituted for the joints of a frame structure to simulate the nonlinear material behaviors of plastic hinges. For vibration control, a separate magnetorheological damper was employed to provide semi-active damping force to the nonlinear structure. A dynamic neural network was designed as a state observer to enable the feedback based semi-active vibration control. Based on the dynamic neural network observer, an adaptive fuzzy sliding mode based output control was developed for the magnetorheological damper to suppress the vibrations of the structure. The performance of the intelligent control algorithm was studied by subjecting the structure to shake table experiments. Experimental results show that the magnetorheological rotary brake can simulate the nonlinearity of the structural model with good repeatability. Moreover, different nonlinear behaviors can be achieved by controlling the input voltage of magnetorheological rotary damper. Different levels of nonlinearity in the vibration response of the structure can be achieved with the above adaptive fuzzy sliding mode control algorithm using a dynamic neural network observer.

**Keywords:** nonlinear structure; vibration control; plastic hinge; intelligent control; dynamic neural network; adaptive fuzzy sliding mode control

---

### 1. Introduction

Structural model design and construction has always played a significant role in structural engineering research, especially in the field of structural control, where the control algorithms and devices need to be verified before they are applied in actual engineering. On the other hand, in nonlinear vibration models of structures, especially when considering material nonlinearity, nonlinear behavior always leads to yielding of or damage to the structure. Therefore, it is very difficult, sometimes impossible, for the model to recover its initial elastic state after each experiment. Therefore, developing a reusable experimental platform for nonlinear structures is very important for nonlinear structural control. Much literature regarding experimentation in structural control is available. Examples of the literature are provided subsequently. Kwak and

---

\*Corresponding author, Professor, E-mail: [gsong@uh.edu](mailto:gsong@uh.edu)

and Sciulli (1996) studied the fuzzy-logic based vibration suppression control of active structures equipped with piezoelectric sensors and actuators. Preumont and Bossens (2000) conducted an experiment regarding active tendon control of truss structure vibration. Battaini *et al.* (2000) introduced a recently developed bench-scale structure control experiment. Yi *et al.* (2001) utilized a six-story test structure to demonstrate the capabilities of multiple MR devices for seismic control of civil engineering structures. Li *et al.* (2005) studied MR damper control of a 3-story frame-shear wall eccentric structure. Ng and Xu (2006) experimented with the possibility of using passive friction dampers to link a podium structure to a main building to resist seismic attacks. Some studies considering the nonlinear behavior of structures have been proposed. Soong (1998) presented a method to use active control forces to simulate the nonlinear behavior of structures. Reynolds and Christenson (2006) utilized disk brakes to simulate elastic-perfectly plastic material behavior to setup a nonlinear bench-scale test structure and employ a shear mode MR damper to control this nonlinear structure.

In this paper, structural nonlinearity was realized by an MR rotary brake, which was used to simulate the plastic hinge of a structure. A one-story, nonlinear model incorporated with a MR rotary brake was designed and constructed. By changing the input voltage to the MR rotary brake, different nonlinear behaviors can be realized. A dynamic neural network (DNN) was designed as a state observer. Based on the DNN observer, an adaptive fuzzy sliding mode based output control was developed for the MR damper to suppress the vibration of the structure. Experimental results show that the MR rotary brake can simulate the nonlinearity of the structural model with good repeatability. Moreover, different nonlinear behaviors can be achieved by controlling the input voltage of MR rotary damper. Response reduction in the vibration of the structure can be realized using the intelligent control algorithms.

## 2. Nonlinear structure model

The MR rotary brake employed in this study to replace a rigid beam-column joint was a compact MR fluid proportional brake (model number RD-2087-01 - Lord Corporation) (Fig.1). A total of two identical MR rotary brakes were used. The total height and width of the structure is 20 inches and 18 inches, respectively. The input of MR rotary brakes is current/voltage signal. Some parameters of the MR rotary brake are shown in Table 1. The current to the MR rotary brake was controlled by a 0-5 Volt DC control signal which was generated by a programmable power supply.



Fig. 1 An MR rotary brake

Table 1 Typical properties of MR rotary brake RD-2087-01(Lord Corporation)

Body Length, mm	~35.7
Body Diameter, mm	96.6
Operating Speed, rpm	120 max
Torque@ 1A, Nm	4
Operating Temperature, °C	-35 to +60

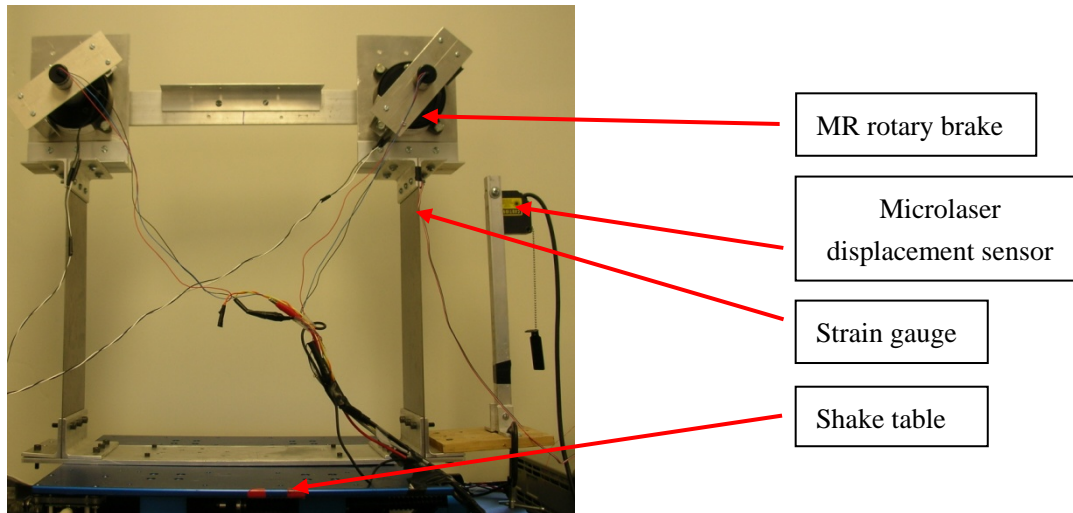


Fig. 2 A nonlinear structure model

A one-story structure model with two identical MR brakes is shown in Fig. 2. The mass of the model structure is 5 kg. The fundamental natural frequency of the original linear structure is 3.3 Hz and the damping ratio is 1%. The sensors adopted here include a micro-laser displacement sensor used to measure the relative displacement of the structure, and a strain gauge to measure the strain of the column in order to determine the moment of the structure using the following equation

$$M(t) = \frac{2EI}{h} \varepsilon(t). \quad (1)$$

where  $E$  is the elastic modulus of steel columns,  $I$  is the second moment of area of steel

columns,  $h$  is the thickness of steel columns and  $\varepsilon(t)$  is the measured strain signals.

The data acquisition system used was a dSPACE data acquisition system with signal input and output capabilities. An Agilent programmable power supply was used to amplify the input to the MR damper. A block diagram of the test system is shown in Fig. 3.

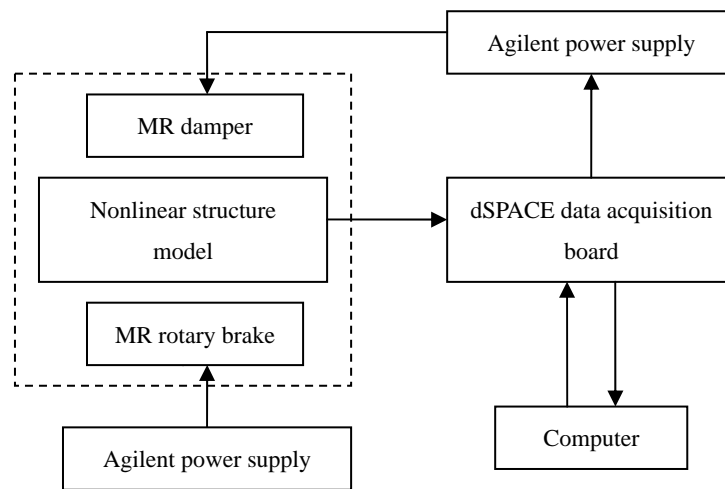


Fig. 3 Block diagram of the nonlinear structure model

### 3. Mechanism of simulating structural nonlinearity

The mechanism of this nonlinear model is described as follows: From its initial (or undeformed) position where the MR rotary brake remains unchanging, the structure begins to vibrate (Fig. 4(a)). At this time, the moment of the hinge is zero. When the strain is in the elastic range, the moment of the hinge is less than the predetermined torque of the MR rotary brake. Therefore, the MR rotary brake does not work (Fig. 4(b)). The strain can still increase; when the strain exceeds the elastic range, the moment of the hinge becomes larger than the predetermined torque of MR rotary brake and the MR rotary brake begins to rotate (Fig. 4(c)). At this time, the joint will change from a rigid connection to a hinged connection and cannot bear more moment.

Through controlling the input voltage to the MR rotary brake, different nonlinear behaviors which are shown in Fig. 5 can be realized. Since the results of two MR brakes are quite similar. Therefore, we only show the results of one MR brake. Through the input of maximum voltage, the linear elastic behaviors can be realized as shown in Fig. 6.

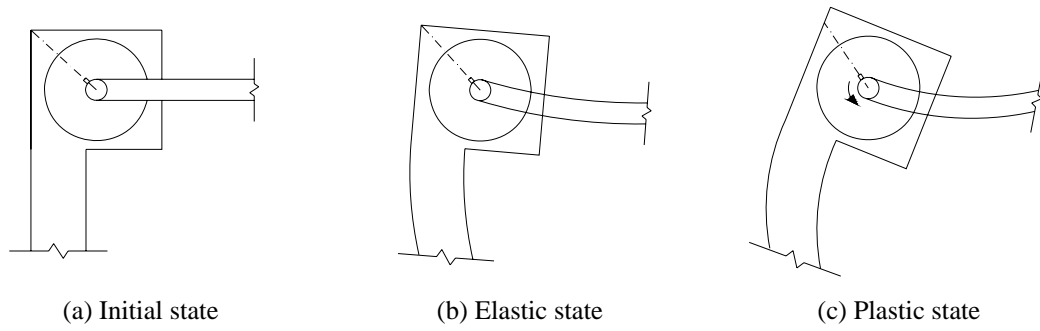


Fig. 4 Typical behavior of MR rotary brake

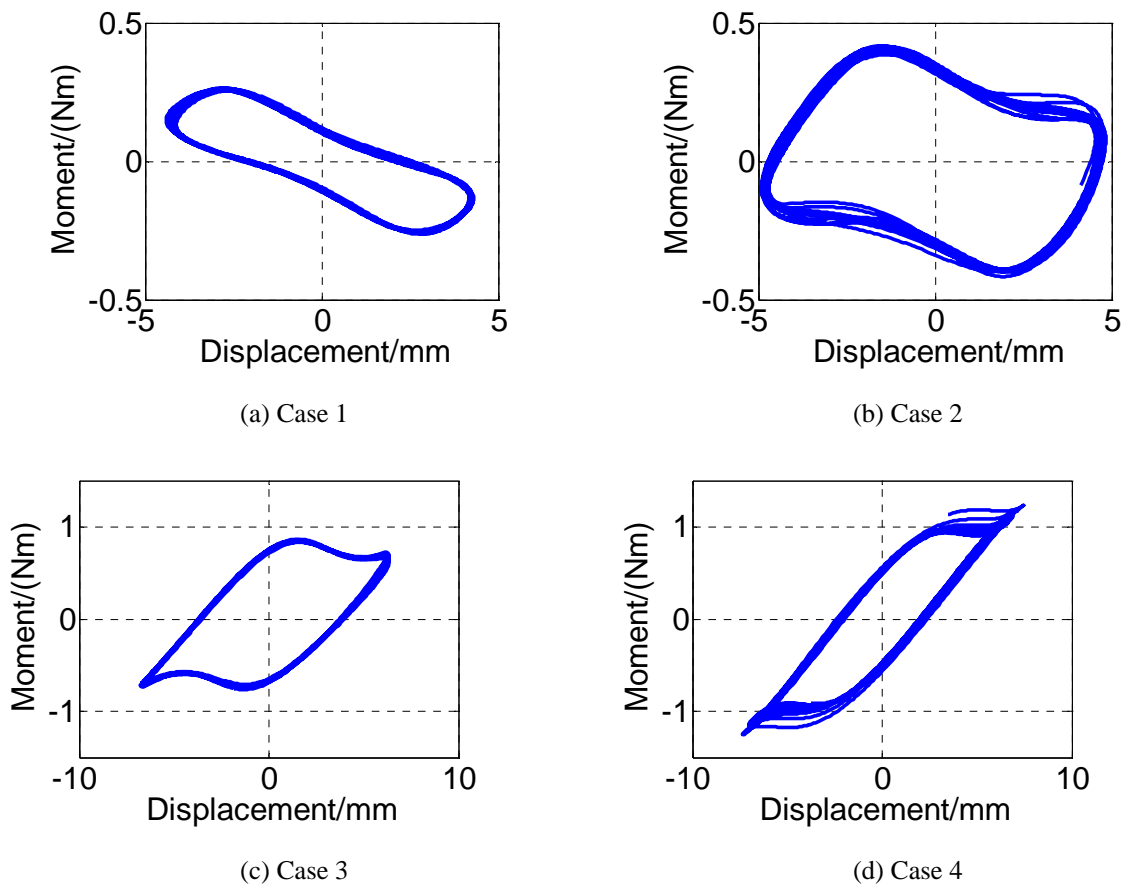


Fig. 5 Different nonlinear behaviors

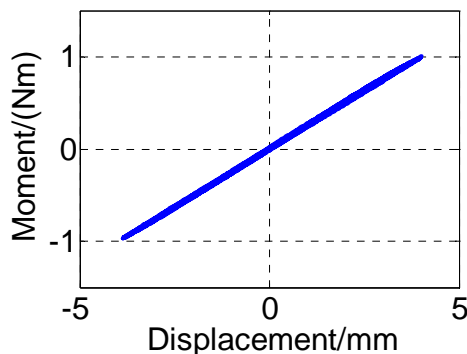


Fig. 6 Linear elastic behavior

From the above figures, all slopes are positive which can be clearly shown from linear elastic one. Some results such as in case 1 and case 2 are like negative slope. The reason is that in these cases the voltage input to the MR rotary dampers is very low. Therefore, the MR rotary dampers will undergo a large plastic behavior, which also means the large displacement of the structure will only cause the small moment of the joint. Thus the shape of the nonlinear behaviors which have positive stiffness is in a flat shape.

#### 4. Intelligent control using MR damper

For nonlinear structural control, the linear based methods can hardly control the vibration. Therefore, in this paper intelligent control algorithms are considered for observer and controller design. MR damper, which has been applied widely in civil engineering, is used in this paper as a semi-active device. In this section, a dynamic neural network based controller is firstly designed to estimate all states of nonlinear structural vibration. According to the states that are obtained from the observer, an adaptive fuzzy sliding mode control is developed to suppress the vibration of nonlinear structure.

##### 4.1 Dynamic neural network (DNN) observer

The nonlinear vibration of structure can be represented by

$$\begin{aligned}\dot{\mathbf{x}} &= \mathbf{f}(\mathbf{x}, \dot{\mathbf{x}}) + \mathbf{B}_u \mathbf{u} \\ \mathbf{y} &= \mathbf{C} \mathbf{x}\end{aligned}\quad (2)$$

where the state vector  $\mathbf{x}$  is a  $n$ -dimensional vector, the input  $\mathbf{u}$  is an  $m$ -dimensional vector, the measured output  $\mathbf{y}$  is a  $q$ -dimensional vector,  $\mathbf{B}_u$  is a  $n \times m$  matrix and  $\mathbf{C}$  is a  $q \times n$  matrix and  $\mathbf{f}(\mathbf{x}, \dot{\mathbf{x}})$  is a  $n$ -dimensional unknown vector function. The problem is to design a state observer for this nonlinear system.

The system (2) can be described by a dynamic neural network as (Fig. 7)

$$\begin{aligned} \dot{\mathbf{x}} &= \mathbf{A}\mathbf{x} + \mathbf{B}\mathbf{W}^*\mathbf{S}(\mathbf{x}) + \mathbf{B}\boldsymbol{\varepsilon}(\mathbf{x}, \mathbf{u}) + \mathbf{B}_u\mathbf{u} \\ \mathbf{y} &= \mathbf{C}\mathbf{x} \end{aligned} \quad (3)$$

where  $\mathbf{A}$  is a  $n \times n$  diagonal matrix,  $\mathbf{B}$  is a  $n \times r$  matrix and  $\mathbf{W}^*$  is a  $r \times L$  matrix of synaptic weights. Finally  $\mathbf{S}(\mathbf{x})$  is an  $L$ -dimensional vector with elements  $s(x_i)$  which are sigmoid functions.  $\boldsymbol{\varepsilon}(\mathbf{x}, \mathbf{u})$  is the model error term with the assumption that  $|\boldsymbol{\varepsilon}(\mathbf{x}, \mathbf{u})| \leq \theta^*$ , where  $\theta^*$  is an unknown constant.

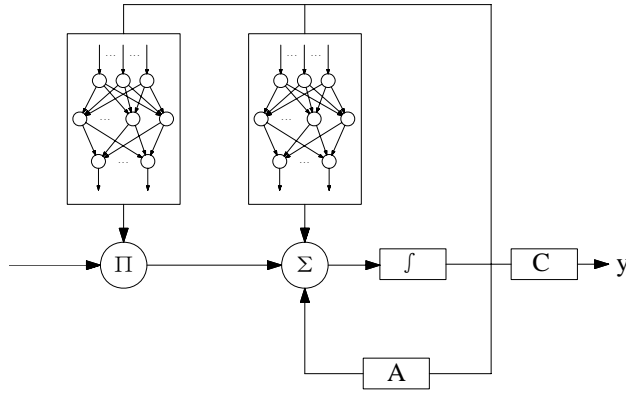


Fig. 7 Block diagram of dynamic neural network

Then the observer that estimates states of the system (2) is

$$\begin{aligned} \dot{\hat{\mathbf{x}}} &= \mathbf{A}\hat{\mathbf{x}} + \mathbf{B}\hat{\mathbf{W}}\mathbf{S}(\hat{\mathbf{x}}) + \mathbf{L}(\hat{\mathbf{y}} - \mathbf{y}) + \mathbf{B}\mathbf{v} + \mathbf{B}_u\mathbf{u} \\ \hat{\mathbf{y}} &= \mathbf{C}\hat{\mathbf{x}} \end{aligned} \quad (4)$$

where  $\hat{\mathbf{x}}$  denotes the estimate of the state  $\mathbf{x}$ ,  $\hat{\mathbf{W}}$  is the estimated value of  $\mathbf{W}^*$ . The estimated error of  $\mathbf{W}^*$  is defined as  $\tilde{\mathbf{W}} = \hat{\mathbf{W}} - \mathbf{W}^*$ .  $\mathbf{L}$  is the gain matrix of the observer. The term  $\mathbf{v}$ , yet to be defined, is a function that provides robustness in the presence of bounded disturbances.

**Lemma:** Consider system (3), the matrix pair  $(\mathbf{A}, \mathbf{C})$  is observable; thus, the gain matrix  $\mathbf{L}$  can be chosen to render matrix  $\mathbf{A}_c = \mathbf{A} + \mathbf{L}\mathbf{C}$  stable. When the matrix pair  $(\mathbf{A}_c, \mathbf{B})$  is controllable, the transfer function matrix  $\mathbf{H}(s) = \mathbf{F}^T \mathbf{C}(s\mathbf{I} - \mathbf{A}_c)^{-1} \mathbf{B}$  is strictly positive real if there exists a  $q \times r$  matrix  $\mathbf{F}$ . Then the only  $n \times n$  positive definite matrix  $\mathbf{P}$  can be found to satisfy

$$\begin{aligned} \mathbf{A}_c^T \mathbf{P} + \mathbf{P} \mathbf{A}_c &= -\mathbf{Q} & \mathbf{P} \mathbf{B} &= \mathbf{C}^T \mathbf{F} \end{aligned}$$

where  $\mathbf{Q}$  is an arbitrary positive definite matrix.

From the Lyapunov stability theory, the training algorithm derived for this neural network is given by

$$\dot{\hat{\mathbf{W}}} = -\gamma \hat{\mathbf{W}} - \mathbf{F}^T \tilde{\mathbf{y}} \mathbf{S}^T(\hat{\mathbf{x}}) \quad (5)$$

$$\dot{\hat{\theta}} = -\gamma_{\theta} \hat{\theta} + |\tilde{\mathbf{y}}^T \mathbf{F}| \quad (6)$$

where  $\gamma, \gamma_{\theta}$  are adaptation gains and the robust control term  $\mathbf{v} = -\hat{\theta} \text{sgn}(\mathbf{F}^T \tilde{\mathbf{y}})$  means  $\mathbf{e}, \tilde{\mathbf{W}}, \tilde{\theta}$  are uniformly and ultimately bounded. The derivation of the above training algorithm is described in Li *et al.* (2006).

Under different nonlinear behaviors, the performance of the DNN observer was verified by experiments (Figs. 8-11). Here, the activation function of the DNN was the sigmoid function and the number of hidden-layer neurons was 2. The adaptation gains  $\gamma, \gamma_{\theta}$  are 3.4 and 0.05 respectively. Matrix  $\mathbf{A}$  was chosen as the state matrix of the linear vibration model of structure and  $\mathbf{B}$  was a vector in which all the elements were 1. The observer gain matrix  $\mathbf{L}$  is computed by a Luenberger observer. The El Centro earthquake wave with peak value scaled to 0.1 g is the input to the shaking table as excitation. The measure output  $\mathbf{y}$  is the displacement of the structure, which is also used as the input for the observer. The different nonlinear behaviors were used based on the above results (Fig. 5).

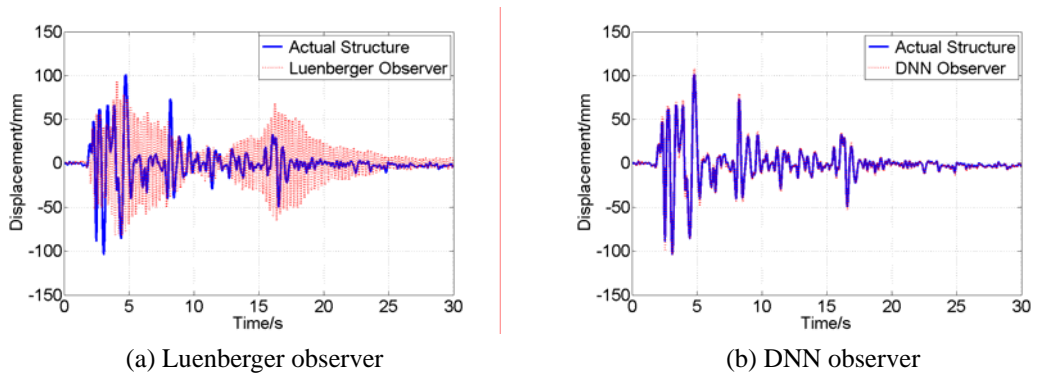
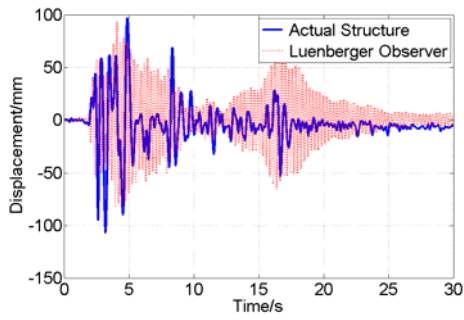
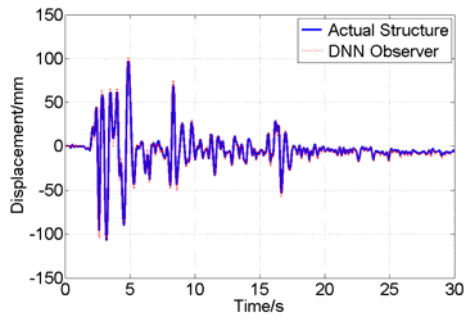


Fig. 8 Observer results under nonlinear case 1

From these figures, it can be seen that the DNN observer can estimate the state of the structure accurately when considering different nonlinear behaviors. However, the Luenberger observer, which is based on a linear model, cannot accurately estimate the state of the structure. These experimental results also verify the conclusion obtained from simulation, which is analyzed in Li *et al.* (2010).

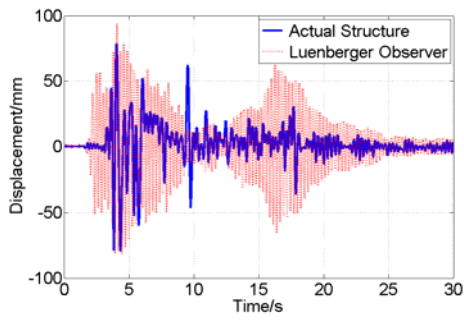


(a) Luenberger observer

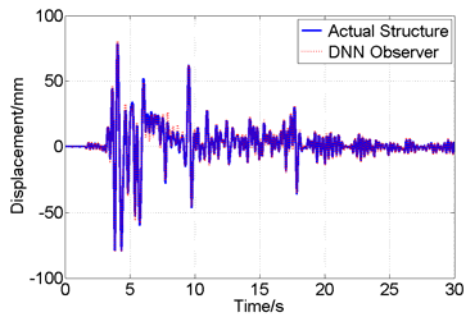


(b) DNN observer

Fig. 9 Observer results under nonlinear case 2

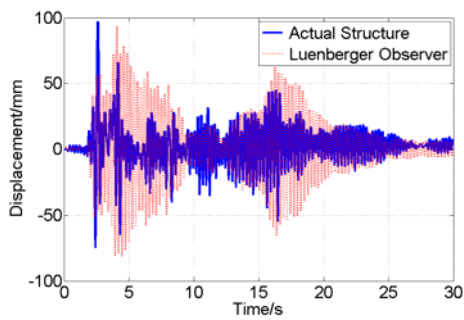


(a) Luenberger observer

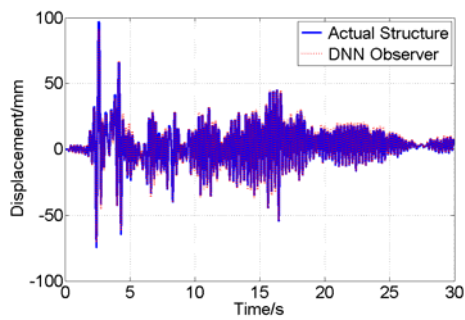


(b) DNN observer

Fig. 10 Observer results under nonlinear case 3



(a) Luenberger observer



(b) DNN observer

Fig. 11 Observer results under nonlinear case 4

#### 4.2 Adaptive fuzzy sliding mode control (AFSM) using DNN observer

The model of a nonlinear structure to be controlled can be expressed as

$$\ddot{x} = f(x, \dot{x}) + \bar{u} + \bar{d} \quad (7)$$

where  $x$  is the displacement of the structure,  $\bar{u}$  is the control input for the structure and  $\bar{d}$  is the external excitation of the structure.

The control force of adaptive fuzzy sliding-mode control is given by the sliding-mode control (Li et al., 2010). According to the arrival condition and the definition of the sliding surface, the sliding-mode control force and sliding surface can be obtained as

$$\bar{u} = -c_1 \dot{x} - f(x, \dot{x}) - (D + \eta) \text{sgn}(s) \quad (8)$$

$$s = c_1 x + \dot{x}, \quad c_1 > 0 \quad (9)$$

where  $c_1$  is a positive constant;  $\eta$  is the adjustable parameter of arrival condition;  $f(x, \dot{x})$  represents the characteristic of nonlinear structure;  $D$  is the upper limit of external excitation;  $s$  is the sliding surface.

Because  $f(x, \dot{x})$  is unknown, the control force shown in Eq. (8) cannot be directly computed.

The reasonable consideration is to substitute  $f(x, \dot{x})$  by a fuzzy system  $\hat{f}(\mathbf{x}|\boldsymbol{\theta}_f)$  so that the sliding-mode control can be used without the characteristic of nonlinear structure beforehand. Moreover, the nonlinear term  $(D + \eta)\text{sgn}(s)$  in the control law yields too many switches in the sliding surface which lead to the chattering phenomenon. Therefore, the other fuzzy system  $\hat{f}(s|\boldsymbol{\theta}_g)$  is introduced to substitute the nonlinear term. Then Eq. (8) can be rewritten as

$$\bar{u} = -c_1 \dot{x} - \hat{f}(\mathbf{x}|\boldsymbol{\theta}_f) - \hat{f}(s|\boldsymbol{\theta}_g) \quad (10)$$

The optimal fuzzy controller parameter vectors are defined as

$$\boldsymbol{\theta}_f^* = \arg \min_{\boldsymbol{\theta}_f \in \Omega_f} \left[ \sup_{\mathbf{x} \in R^2} \left| \hat{f}(\mathbf{x}|\boldsymbol{\theta}_f) - f(x, \dot{x}) \right| \right] \quad (11)$$

$$\boldsymbol{\theta}_g^* = \arg \min_{\boldsymbol{\theta}_g \in \Omega_g} \left[ \sup_{s \in R} \left| \hat{f}(s|\boldsymbol{\theta}_g) - (D + \eta) \text{sgn}(s) \right| \right] \quad (12)$$

where  $\Omega_f$  is the constrain set of  $\theta_f$ ;  $\Omega_s$  is the constrain set of  $\theta_s$ ,

The minimum approximate error is defined as

$$\omega = f(x, \dot{x}) - \hat{f}(\mathbf{x}|\theta_f^*) + (D + \eta)\text{sgn}(s) - \hat{f}(s|\theta_s^*) \quad (13)$$

Specifically, using the product inference engine, singleton fuzzifier, and center average defuzzifier, the fuzzy system can be expressed as

$$f(\mathbf{x}|\theta) = \theta^T \xi(\mathbf{x}) \quad (14)$$

where  $\theta \in R^{\prod_{i=1}^2 m_i}$  consists of the adjustable parameter  $\bar{y}_u^{-l_2}$ ;  $\xi(\mathbf{x})$  is defined as

$$\xi^{l_1 l_2}(\mathbf{x}) = \frac{\prod_{i=1}^2 \mu_{A_i^{l_i}}(x_i)}{\sum_{l_1=1}^{m_1} \sum_{l_2=1}^{m_2} \left( \prod_{i=1}^2 \mu_{A_i^{l_i}}(x_i) \right)}$$

$l_1$  and  $l_2$  of which the maximum value are  $m_1$  and  $m_2$  are the index numbers for the fuzzy rules, respectively.  $\mu_{A_i^{l_i}}(x_i)$  is the fuzzy membership function of linguistic variable,  $A_i^{l_i}$ , which is defined for the  $i$ th input.  $\bar{y}_u^{-l_2}$  is the point at which the fuzzy membership function for output achieves its maximum value of the corresponding fuzzy rule.

From Eqs. (7), (9), (13) and (14), we have

$$\begin{aligned} \dot{s} &= f(x, \dot{x}) - \hat{f}(\mathbf{x}|\theta_f) + \bar{d}(t) - \hat{f}(s|\theta_s) \\ &= \hat{f}(\mathbf{x}|\theta_f^*) - \hat{f}(\mathbf{x}|\theta_f) + \hat{f}(s|\theta_s^*) - \hat{f}(s|\theta_s) + \omega + \bar{d}(t) - (D + \eta)\text{sgn}(s) \\ &= \boldsymbol{\varphi}_f^T \xi(\mathbf{x}) + \boldsymbol{\varphi}_s^T \psi(s) + \omega + \bar{d}(t) - (D + \eta)\text{sgn}(s) \end{aligned} \quad (15)$$

where  $\boldsymbol{\varphi}_f = \theta_f^* - \theta_f$ ,  $\boldsymbol{\varphi}_s = \theta_s^* - \theta_s$ . The Lyapunov function can be chosen as

$$V = \frac{1}{2} \left( s^2 + \frac{1}{\gamma_1} \boldsymbol{\varphi}_f^T \boldsymbol{\varphi}_f + \frac{1}{\gamma_2} \boldsymbol{\varphi}_s^T \boldsymbol{\varphi}_s \right) \quad (16)$$

where  $\gamma_1$  and  $\gamma_2$  are positive constants. The differentiation of Eq. (16) is

$$\begin{aligned} \dot{V} &= s\dot{s} + \frac{1}{\gamma_1} \boldsymbol{\varphi}_f^T \dot{\boldsymbol{\varphi}}_f + \frac{1}{\gamma_2} \boldsymbol{\varphi}_s^T \dot{\boldsymbol{\varphi}}_s \\ &= s \left[ \boldsymbol{\varphi}_f^T \xi(\mathbf{x}) + \boldsymbol{\varphi}_s^T \psi(s) + \omega + \bar{d}(t) - (D + \eta)\text{sgn}(s) \right] + \frac{1}{\gamma_1} \boldsymbol{\varphi}_f^T \dot{\boldsymbol{\varphi}}_f + \frac{1}{\gamma_2} \boldsymbol{\varphi}_s^T \dot{\boldsymbol{\varphi}}_s \end{aligned}$$

$$\begin{aligned}
&= s\boldsymbol{\phi}_f^T \boldsymbol{\xi}(\mathbf{x}) + \frac{1}{\gamma_1} \boldsymbol{\phi}_f^T \dot{\boldsymbol{\phi}}_f + s\boldsymbol{\phi}_s^T \boldsymbol{\psi}(s) + \frac{1}{\gamma_2} \boldsymbol{\phi}_s^T \dot{\boldsymbol{\phi}}_s + s\omega + s\bar{d}(t) - (D + \eta)|s| \\
&< s\boldsymbol{\phi}_f^T \boldsymbol{\xi}(\mathbf{x}) + \frac{1}{\gamma_1} \boldsymbol{\phi}_f^T \dot{\boldsymbol{\phi}}_f + s\boldsymbol{\phi}_s^T \boldsymbol{\psi}(s) + \frac{1}{\gamma_2} \boldsymbol{\phi}_s^T \dot{\boldsymbol{\phi}}_s + s\omega + |s|D - (D + \eta)|s| \\
&= \frac{1}{\gamma_1} \boldsymbol{\phi}_f^T [\gamma_1 s \boldsymbol{\xi}(\mathbf{x}) + \dot{\boldsymbol{\phi}}_f] + \frac{1}{\gamma_2} \boldsymbol{\phi}_s^T [\gamma_2 s \boldsymbol{\psi}(s) + \dot{\boldsymbol{\phi}}_s] + s\omega - \eta|s|
\end{aligned} \tag{17}$$

where  $\dot{\boldsymbol{\phi}}_f = -\dot{\boldsymbol{\theta}}_f$ ,  $\dot{\boldsymbol{\phi}}_s = -\dot{\boldsymbol{\theta}}_s$ . Then we can obtain the adaptation law as

$$\dot{\boldsymbol{\theta}}_f = \gamma_1 s \boldsymbol{\xi}(\mathbf{x}) \tag{18}$$

$$\dot{\boldsymbol{\theta}}_s = \gamma_2 s \boldsymbol{\psi}(s) \tag{19}$$

The control inputs, namely, the total states of the structure, are estimated by the DNN observer verified by the above experiment. The experimental model with MR damper is shown in Fig. 12. On the underside of the frame, a steel tongue is rigidly attached. The steel tongue leads downwards, with the opposite end dipped into a small MR fluid reservoir damper mounted on the rigid base. A toroidal electromagnet is placed around the MR fluid reservoir damper such that the terminating ends of the electromagnet can control the MR reservoir damper through the input voltage to the electromagnet.

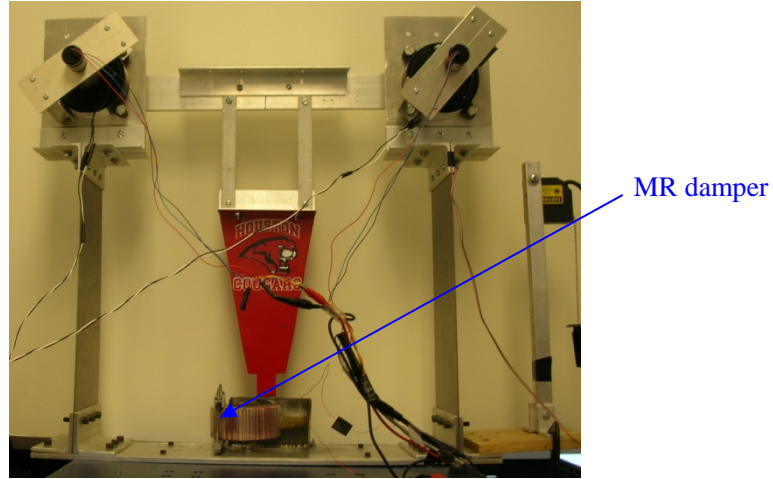


Fig. 12 The experimental model with an MR damper

Under different nonlinear behaviors, experiments using AFSM control were conducted. The states used to compute the force were estimated by the DNN observer. The control effect and control signal are shown as Figs. 13-16.

From the above experimental data, it is clear that the proposed control was effective in vibration

suppression under different behaviors of the nonlinear structural model. Therefore, the AFSM control proposed before is also suitable for the control of nonlinear vibrations in a model structure.

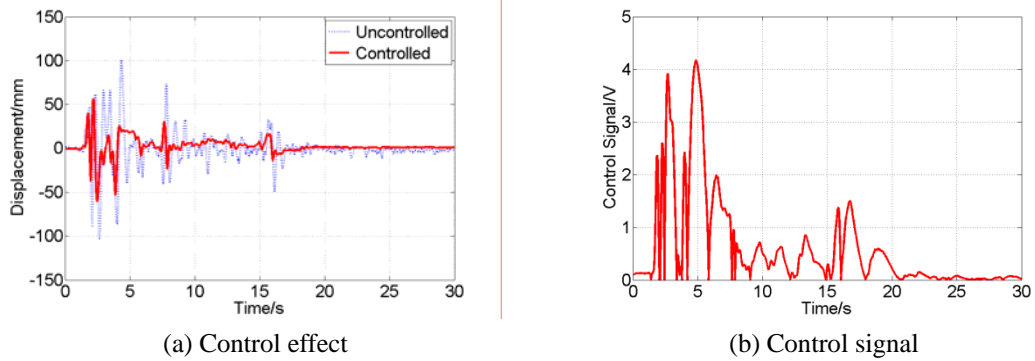


Fig. 13 Control results under nonlinear case 1

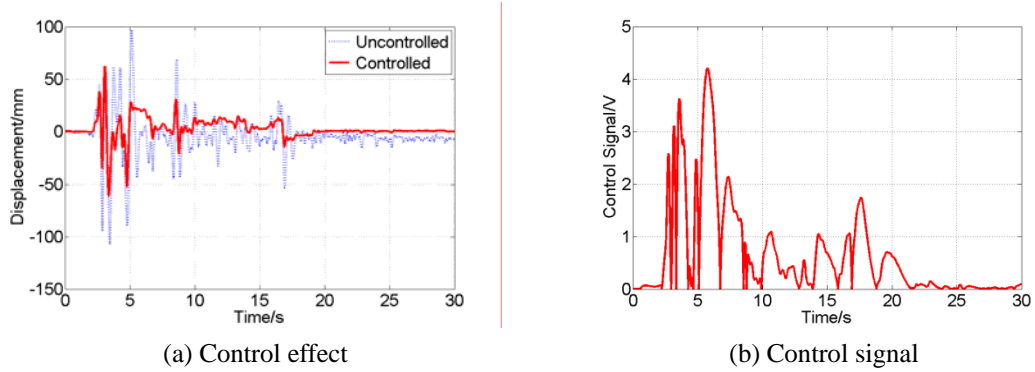


Fig. 14 Control results under nonlinear case 2

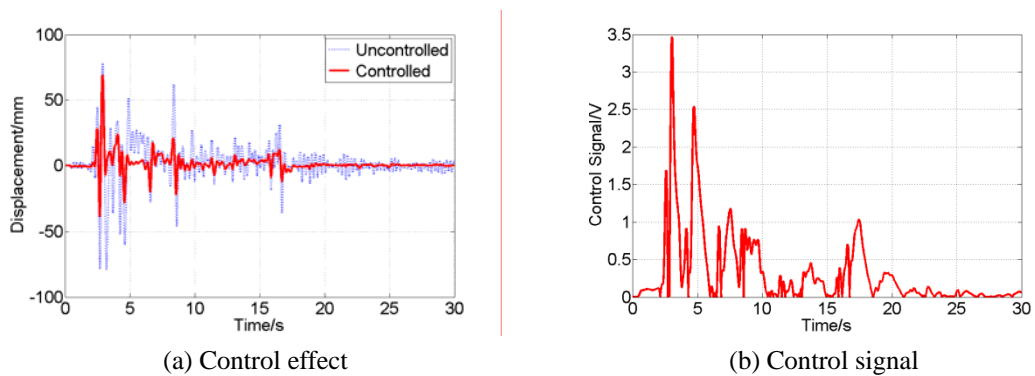


Fig. 15 Control results under nonlinear case 3

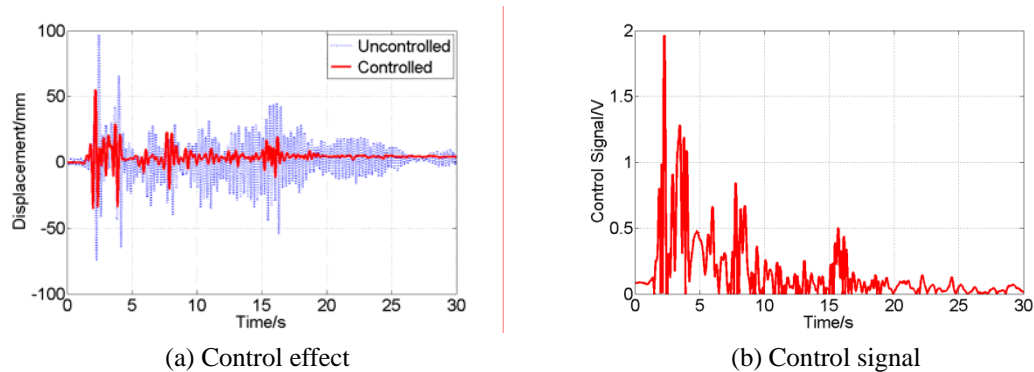


Fig. 16 Control results under nonlinear case 4

## 5. Conclusions

In this paper, a one-story nonlinear structure model was developed and used to verify the proposed intelligent vibration control algorithm. The nonlinear structural model was equipped with MR rotary brakes, and different nonlinear behaviors were realized by controlling the input voltage to the MR rotary brakes. To facilitate vibration control of the nonlinear structure, a separate MR damper was used and a DNN observer was designed to estimate the states. Experimental results show that the DNN can accurately estimate the state of the nonlinear vibration. On the other hand, the Luenberger observer, which was designed based on a linear model, cannot accurately estimate the state of the nonlinear structure. Experimental results also verify the effectiveness of the DNN observer based adaptive fuzzy sliding mode control for vibration suppression of the nonlinear frame structure.

## 6. Acknowledgments

This work was partially supported by the National Science Foundation of USA under Award No. 0442991 and Award No. 0602508, the Fundamental Research Funds for the Central Universities under Award No. DUT11RC(3)01, the National Science Foundation of China (NSFC) under Award No. 50908033, and the Science Fund for Creative Research Groups of the NSFC under Award No. 51121005.

## References

Battaini, M. Yang, G. and Spencer Jr., B.F. (2000), "Bench-scale experiment for structural control", *J. Eng.*

- Mech. - ASCE*, **126**(2), 140-148.
- Harris, H.G., Sabnis, G.M. and White, R.N. (1999), *Structural modeling and experimental techniques*, CRC Press.
- Kwak, M.K. and Sciulli, D. (1996), "Fuzzy-logic based vibration suppression control experiments on active structures", *J. Sound Vib.*, **191**(1), 15-28.
- Li, L.Y. and Ou, J.P. (2006a), "Magnetorheological damper control and simulation analysis for vibration reduction of nonlinear structure based on AFSMC algorithm", *Earthq. Eng. Vib.*, **26**(2), 96-103
- Li, L.Y. and Ou, J.P. (2006b), "Adaptive fuzzy sliding mode control for nonlinear vibration reduction of structure", *J. Vib. Eng.*, **19**(3), 319-325.
- Li, L.Y. and Ou, J.P. (2006c), "Dynamical neural network observer design for the nonlinear vibration model of structure", *Proceedings of the 4<sup>th</sup> China-Japan-US Symposium of Structural Control and Monitoring*, Hangzhou, China.
- Li, L.Y., Song, G. and Ou, J.P. (2010), "Nonlinear structural vibration suppression using dynamic neural network observer and adaptive fuzzy sliding mode control", *J. Vib. Control*, **16**(10), 1503-1526.
- Li, X.L. and Li, H.N. (2005), "Experiment study control of frame-shear wall eccentric structure using MRD", *J. Harbin Inst. Technol.*, **37**(3), 147-150.
- MR Rotary Brake RD-2087-01. Lord Corporation.
- Ng, C.L. and Xu, Y.L. (2006), "Seismic response control of a building complex utilizing passive friction damper: experimental investigation", *Earthq. Eng. Struct. D.*, **35**(6), 657-677.
- Ohtori, Y. Christenson, R.E. Spencer Jr., B.F. and Dyke, S.J. (2004), "Benchmark control problems for seismically excited nonlinear buildings", *J. Eng. Mech. - ASCE*, **130**(4), 366-385.
- Preumont, A. and Bossens, F. (2000), "Active tendon control of vibration of truss structures: theory and experiments", *J. Intell. Mater. Syst. Struct.*, **11**(2), 91-99.
- Reynolds, W.E. and Christenson, R.E. (2006), "Bench-scale nonlinear test structure for structural control research", *Eng. Struct.*, **28**, 1182-1189.
- Soong, T.T. (1998), "Experimental simulation of degrading structures through active control", *Earthq. Eng. Struct. D.*, **27**(2), 143-154.
- Tse, T. and Chang, C.C. (2004), "Shear-mode rotary magnetorheological damper for small-scale structural control experiments", *J. Struct. Eng. - ASCE*, **130**(6), 904-911.
- Yi, F., Dyke, S.J., Caicedo, J.M. and Carlson, J.D. (2001), "Experimental verification of multiinput seismic control strategies for smart dampers", *J. Eng. Mech. - ASCE*, **127**(11), 1152-1164.